Available online at www.sciencedirect.com
SCIENCE DIRECT®
Bioorganic & Medicinal Chemistry 12 (2004) 5057–5062
Bioorganic & Medicinal Chemistry

Designed calix[8]arene-based ligands for selective tryptase surface recognition

Tommaso Mecca, Grazia M. L. Consoli, Corrada Geraci and Francesca Cunsolo*

Istituto di Chimica Biomolecolare (sez. di Catania), CNR, Via del Santuario 110, I-95028 Valverde (CT), Italy

Received 9 June 2004; revised 13 July 2004; accepted 16 July 2004
Available online 20 August 2004

Abstract—Basic amino acid calix[8]arene receptors for tryptase surface recognition have been synthesized. The tetrameric arrangement and the negative charge distribution close to the active sites of the enzyme, have suggested the design of complementary multifunctional receptors that might bind to the active region of the protein blocking the approach of the substrate. Kinetic inhibition analysis on recombinant lung tryptase have showed a time-dependent competitive inhibition with both initial and steady-state rate constants in the nanomolar range.

1. Introduction

Design and realization of synthetic receptors able to recognize protein surfaces is an emerging field of interest for bioorganic chemists.[1] This approach offers a valid alternative way to the discovery of nonconventional enzyme inhibitors,[2] and provides useful tools to probe into the protein–protein interactions which represent the key of relevant biological processes.[3–8]

Each protein has its own exterior surface being characterized by a peculiar pattern of amino acid residues. This unique distribution of functional groups could lead to the complementary receptors design having effective and selective protein recognition capabilities.

Herein we report the synthesis of new surface receptors with potent and selective inhibition activity for both human and recombinant lung β-tryptase.

2. Result and discussion

2.1. Tryptase structure

Tryptase is the predominant serine protease of human mast cell,[9,10] playing an important role in the pathogenesis of asthma[11] and other allergic and inflammatory disorders such as conjunctivitis and psoriasis.[12] As a result, inhibitors of human tryptase are becoming of potential therapeutic value in the treatment of various disorders.[13]

Recently, the X-ray crystal structure (3 Å resolution) of human lung tryptase has been reported, highlighting the unique shape of this enzyme.[14,15] It is a square ring, formed by four quasi-equivalent monomers, enzymatically active only as a tetramer kept together by heparin. In the absence of heparin (or of high salt concentration, in vitro) tryptase rapidly dissociates into inactive monomers.[16–18] The four active centers of the tetramer are directed towards a central oval hole measuring approximately 50 Å × 30 Å. Although the amino acid sequence and the folded shape of the tryptase monomers show several identities with the other serine proteases like trypsin or chymotripsin, in the tetrameric active form it is quite resistant to most proteinase inhibitors. Up to now, only a naturally occurring leech-derived tryptase inhibitor (LDTI) has been reported, showing a 50% inhibition of the cleavage activity toward chromogenic substrates, but a lack of selectivity to trypsin and chymotripsin.[19] Several synthetic inhibitors have been proposed and a lot of them contain one or more amidino or guanidino groups that direct the interaction forming a 'salt bridge' with the aspartic acid residue at 189 inside the active pocket of β-tryptase. Some of these have been investigated in clinical trials for the treatment of asthma, psoriasis and ulcerative colitis.[12,20,21] Due to the particular tetrameric arrangement, is also conceivable to design and synthesize selective multifunctional

Keywords: Synthetic receptors; Molecular recognition; Calixarenes; Enzyme inhibitors.
* Corresponding author. Tel.: +39-095-7212136; fax: +39-095-7212141; e-mail: francesca.cunsolo@icb.cnr.it

0968-0896/$ - see front matter © 2004 Elsevier Ltd. All rights reserved.
doi:10.1016/j.bmc.2004.07.037

inhibitors able to span the gap between the four associated subunits. Till now only some bifunctional dibasic inhibitors have been reported.[22] Moreover, each monomer shows an uneven distribution of charges along the molecular surface with negatively charged residues (Asp 143, Asp 145, and Asp 147) clustered preferentially on the inner pore-facing surface, near the active site cleft (Fig. 1).[14,15] These negative clusters could also represent an anchoring point for multifunctional surface inhibitors able to sterically block the substrate docking into the active sites.

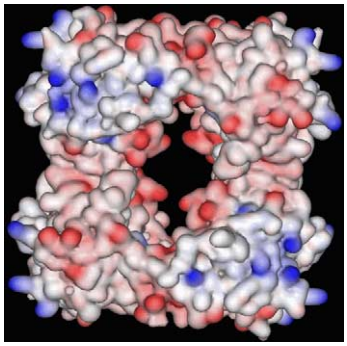

Figure 1. Solid-surface representation of X-ray crystal structure of human tryptase tetramer (Protein Data Bank code 1A0L). The colors indicate positive (blue) and negative (red) electrostatic potential at the molecular surface.

2.2. Chemistry

Our strategy to carry out complementary multifunctional surface inhibitors, was to use as molecular scaffold a calix[8]arene to which eight basic amino acid residues can be attached.

p-tert-Butylcalix[8]arene[23] **1** is a readily available compound with pleated loop shape and external diameter of about 18 Å.

It is a mobile molecule showing a good reactivity to both functions on the upper and lower rim of the macrocycle.[24]

Choosing the suitable amino acid, it is possible to obtain a coupled amino acid calixarene derivative with shape, dimension, and charge distribution, able to fit into the active sites-defined hole of the enzyme. The building block octaminocalix[8]arene derivative **2** was obtained by exhaustive alkylation of the phenolic functions (NaH, PrI) of **1** followed by *ipso*-nitration to the upper rim (CH_3COOH, HNO_3) and reduction (H_2, Pd/C) of the nitric groups to amino.[25] Subsequent coupling (DCC, HOBT in DMF) with Boc-protected amino acids, followed by deprotection with TFA, gave saline derivatives **3**–**6**.

Derivatives **3**–**6** are still conformationally mobile molecules keeping preferentially a quasi-flat shape. CPK models, assuming for these compounds a quasi-circular conformation, indicated a maximum diameter from 30 to 40 Å going from the smaller to the larger derivatives. Besides this, a positive charged area surrounds the external edge of the molecule.

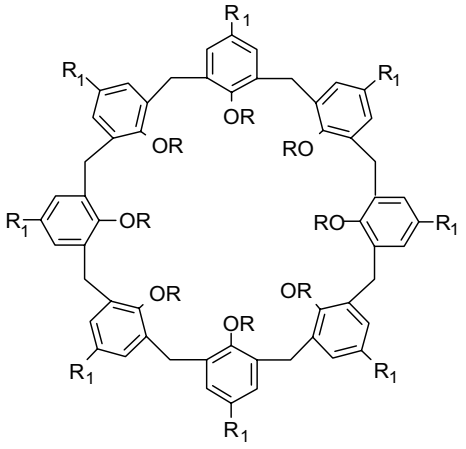

1 R = H $R_1 = C(CH_3)_3$
2 R = Pr $R_1 = NH_2$
3 R = Pr $R_1 = NHCO(CH_2)_2NH_2$
4 R = Pr R_1 = NHLys
5 R = Pr $R_1 = NHCO(CH_2)_5NH_2$
6 R = Pr $R_1 = NHCO(CH_2)_7NH_2$

2.3. Kinetic experiments

Inhibition experiments, carried out on human lung tryptase with saline derivatives **3**–**6** according to the procedures of Schwartz and Bradford,[17] showed a rapid inactivation of the enzyme that seemed to be independent both by the type and derivatives concentration.

This unclear behavior prompted us to suppose that a strong interaction between the poly-positive-charged calixarene derivatives and the poly-negative-charged heparin used to stabilize the enzyme in the active tetrameric form took place.[26] In fact, all derivatives **3**–**6**, in the same experimental kinetic condition, yielded a white insoluble precipitate due to the formation of an inactive complex between derivatives **3**–**6** and heparin. Therefore, heparin stabilized tryptase inactivation is ascribed to the heparin antagonist effect of derivative **3**–**6**.

To overcome this problem and understand whether enzyme recognition by complementary surface interaction is also possible, we decided to use a recombinant human tryptase (rHT) expressed in *Pichia pastoris*.[27]

This enzyme is commercially available heparin-free, stabilized in the tetrameric form by a high concentration of NaCl (2 N). Kinetic experiments to determine the inhibition parameters, were carried out without preincubation of the enzyme–inhibitor solution[28] because, in the absence of heparin, the stability and the enzymatic activity of tryptase were crucially affected.[16–18]

Thus, kinetic assays (at 25 °C) were started by adding the recombinant enzyme to a Tris–HCl buffer (pH 8), containing fixed concentration of Tosyl-Gly-Pro-Arg-*p*-nitroanilide (GPR-*p*NA, 240 μM) as chromogenic sub-

strate, NaCl (0.1 M), and inhibitor **4** at different concentrations. The rate of hydrolysis of the 4-nitroanilide substrate by increasing of absorbance at 405 nm was monitored (Fig. 2). In the absence of inhibitor, time course was linear for at least 30 min. In the presence of the inhibitor, the resulting curves showed a nonlinear concave-down progress which was consistent with a slow binding or time-dependent enzyme inhibition by derivative **4**.

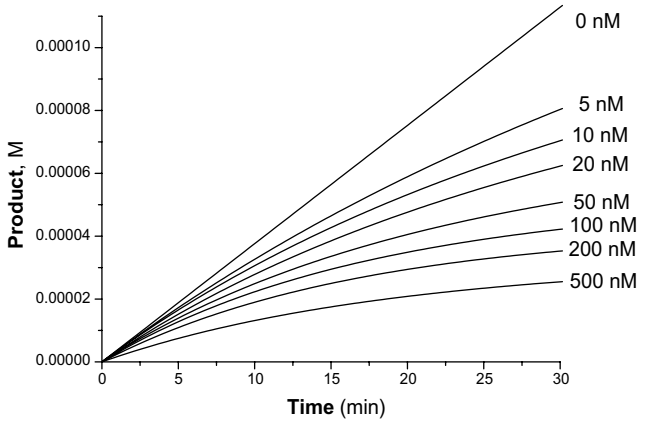

Figure 2. Progress curves of product formation illustrating time-dependent inhibition of recombinant tryptase by the indicated concentrations of derivative **4**.

Time-dependent inhibition can be distinguished into three general kinetic mechanisms: (i) the simple reversible slow binding mechanism, represented by the following equation, where E represent the enzyme and I is a classical inhibitor that binds the enzyme with a slow rate:

$$E \underset{K_2}{\overset{K_1[I]}{\rightleftarrows}} EI$$

(ii) an enzyme isomerization mechanism, where the inhibitor–enzyme binding occurs with the rapid formation of an initial collision complex that undergoes a slow isomerization, as shown in the following equation:

$$E \underset{K_2}{\overset{K_1[I]}{\rightleftarrows}} EI \underset{K_4}{\overset{K_3}{\rightleftarrows}} E^*I$$

and (iii) a third mechanism associated with irreversible enzyme inactivation due to a covalent bonding between the enzyme and some reactive group of the inhibitor.

The second mechanism is regulated by two different inhibition constants. The first (K_i) related to the early EI complex, and the second (K_i^*) for the isomerized enzyme–inhibitor complex E^*I. The progress curves obtained during kinetic experiments at different concentration of calixarene inhibitor **4** (Fig. 2), can be described by the following equation:

$$P = v_s t + (v_0 - v_s)[1 - \exp(-k_{obs} t)]/k_{obs}$$

where P is the concentration of products, v_s and v_0 are the initial and steady state velocities, respectively, k_{obs} is an apparent first order constant, and t is the time.[29]

Nonlinear regression fitting of the curves, using the Marquardt–Levenberg algorithm incorporated in ORIGIN software, gave the values for initial velocity (v_0), final steady-state velocity (v_s), and k_{obs}.

Following the procedure described by Morrison and Walsh,[30] the initial enzyme velocity (v_0), was plotted as a function of inhibitor concentration, the data were fit to the equation $v_0 = V_{max}[S]/\{K_m(1+[I]/K_i)+[S]\}$ and the initial inhibition constant K_i was obtained. In a similar way, the steady-state rate velocity, v_s, was plotted as a function of inhibitor concentration, the data were fit to the equation $v_s = V_{max}[S]/\{K_m(1 + [I]/K_i^*) + [S]\}$ and the steady-state inhibition constant K_i^* was obtained (Fig. 3).

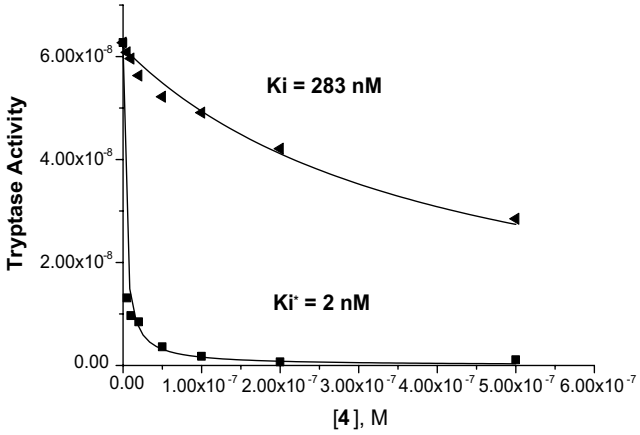

Figure 3. Plots of v_0 (▲) and v_s (■) data to obtain K_i and K_i^*, respectively, for derivative **4**.

Similar kinetic experiments were carried out with the other derivatives **3**, **5**, and **6** that exhibited a slow binding inhibition too. The initial (K_i) and steady-state (K_i^*) inhibition rate constants were determined. The results for inhibition of rHT by each receptor are summarized in Table 1.

Table 1. Rate constants for the inhibition of rHT by derivative **3**–**6**

Compounds	K_i (nM)	K_i^* (nM)
3	582 ± 20	77 ± 1.5
4	283 ± 15	2 ± 0.3
5	99 ± 10	6 ± 0.6
6	626 ± 50	79 ± 2

These results highlighted the better inhibition capability of **4** and **5** with respect to **3** and **6**. Thus, because there was a very close structural likeness among all derivatives, this different behavior indicated a remarkable distance-defined structure–activity relationship, reasonable for this tetrameric enzyme in which the fitting of the surface inhibitor inside the pore could be crucial. Moreover, the better results showed by K_i^* values for receptor **4**, could be explained as a consequence of the increased positive charged area on the macrocyclic scaffold with respect to the same-size derivative **5**. Correlation of the k_{obs} value (obtained from the fitting of each curve

of Figure 2) against [**4**] gave a nonlinear plot that is consistent with slow binding inhibition through a two-step enzyme isomerization mechanism (Fig. 4).

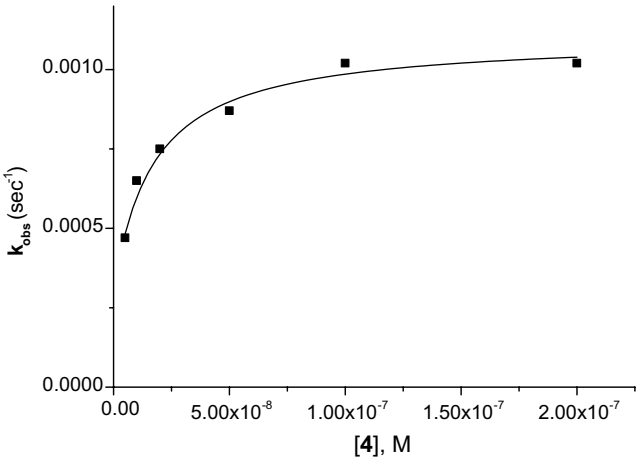

Figure 4. Plot of k_{obs} against [**4**].

Moreover, to realize if inhibition was competitive, noncompetitive or uncompetitive, measures of dependence of k_{obs} on substrate concentration, at fixed enzyme and inhibitor concentrations were made. With derivative **4**, k_{obs} decreases with the increase of substrate concentration, indicating a competitive mode of interaction with the enzyme (Fig. 5).

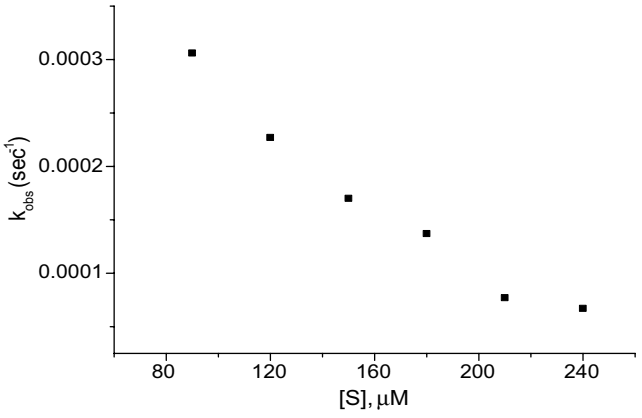

Figure 5. Plot of k_{obs} against [GPR-*p*NA] at fixed concentration of tryptase and **4**.

The latter observation supported the hypothesis that the surface complementary receptors interacting in a very close area to the enzymatic active sites, barred the approach way of the substrate (Fig. 6).

Previous studies on similar water-soluble calixarene derivatives had evidenced the possibility to form micellar aggregates.[31] Because it could widely influence the interaction mode between enzyme and the calixarene inhibitors, solutions at different concentrations of derivative **4**, in Tris–HCl buffer at pH 8, in the presence of NaCl, were tested by quasi-elastic light-scattering (QELS) measurements. These experiments, carried out in a range of concentrations between 10^{-3} and 10^{-6} M

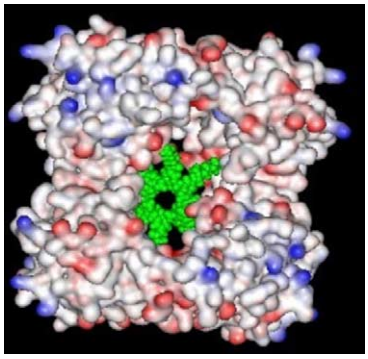

Figure 6. Proposed representation for the complex between tryptase and inhibitor **4** (green CPK model).

pointed out that only a 0.001% of molecules produced aggregates with a hydrodynamic radius of $R_H = 500$ Å. This result make sure about the high prevalence in solution of monomeric species.

3. Conclusion

In conclusion, appropriate functionalization of the calix[8]arene scaffold, furnished a new type of tryptase inhibitors. Human tryptase was indirectly inhibited due to the antagonist effect of derivative **3**–**6** on the proteoglycan heparin. At the same time, competitive inhibition of rHT was also achieved supporting the effectiveness of these surface binding receptors that could outline a new approach to the design of artificial enzymatic inhibitors. Trypsin, another serine protease, showed no inhibition by derivative **4**, underlining its selectivity for tryptase.

Although the high molecular weight makes these derivatives fairly unattractive as drug candidates, they could have potential utility as novel tools to better understand how tryptase is involved in protein–protein interactions.

A more in-depth study about the recognition phenomenon of derivatives **3**–**6** toward heparin, is now under investigation. The cluster of positive charge exposed by these basic derivatives makes them, to the best of our knowledge, the first class of nonproteic and nonpolymeric derivative heparin binders.

4. Experimental

4.1. General comments

All chemicals were reagent grade and used without further purification. *p-tert*-Butylcalix[8]arene **1** was prepared following literature procedures.[32] Heparin-stabilized human lung tryptase and Tosyl-Gly-Pro-Arg-*p*-nitroanilide (GPR-*p*NA) were purchased from Sigma. Recombinant lung β-Tryptase was purchased from Promega. ^{1}H NMR spectra were acquired at 400.13 MHz on a Bruker Avance™400. The acquisition conditions (temperature and solvents used) are specified whenever required. ESI-MS spectra were acquired under positive ionization conditions on a Waters-Micromass

ZQ2000. UV spectra were acquired on a Agilent 8453 UV–vis spectrophotometer equipped with a multicell transport sampling system (eight cells).

4.2. Preparation of 2

A suspension of *p-tert*-butylcalix[8]arene **1** (10 g, 7.71 mmol) in DMF was stirred until a clear solution was obtained (20 min). Then NaH (1.850 g, 77.1 mmol) was added and stirring was continued for 20 min. After addition of PrI (13 g, 7.52 mL, 77.1 mmol) the reaction mixture was stirred at room temperature overnight. Solvent was removed under vacuum to leave a residue which was suspended in 0.1 N HCl (30 mL). The insoluble material was collected by filtration, washed with MeOH (10 mL) and dried to give octa-*tert*-butyl-octa-*O*-propoxycalix[8]arene **1a** (12 g, 96 % yield). *ipso*-Nitration of derivative **1a** was performed by treatment with HNO_3/CH_3COOH, in CH_2Cl_2 at room temperature, using the procedure reported for calix[4]arene.[25] The crude reaction mixture was suspended in acetone and the pure octa-nitro-octa-*O*-propoxycalix[8]arene derivative **1b** was precipitated as white solid (40% yield). Compound **1b** was dissolved in methanol/ethyl acetate and catalytic amount of Pd/C was added. The mixture was stirred under H_2 (2 bar) at rt for 24 h. The catalyst was removed and the filtrated was evaporated to give the corresponding octamino derivative **2** (90%). ^{1}H NMR data for compound **2**: (400 MHz, $CDCl_3$, 297 K) δ 0.98 (t, $J = 7.3$ Hz, 24H), 1.76 (q, $J = 6.8$ Hz, 16H), 3.28 (br s, 16H), 3.69 (t, $J = 6.5$ Hz, 16H), 3.86 (s, 16H), 6.17 (s, 16H).

4.3. General procedure for octa-aminoacid calix[8]arene synthesis (3–6)

N-Boc-aminoacid (1.2 mmol) and HOBT (1.4 mmol) in 5 mL of dry DMF were stirred in a round flask at room temperature DCC (1.3 mmol) and, after 15 min, derivative **2** (0.1 mmol), in 2 mL of dry DMF were added. The reaction was stirred for 3 h. The solvent was removed and reaction mixture was purified by flash chromatography on silica gel using a gradient of CH_2Cl_2/EtOH, from 98:2 to 94:6. Yield of the coupling reactions is nearly to 80% with all the amino acids used. Further treatment with TFA at room temperature for 1 h, gave saline derivative **3**–**6**.

4.3.1. Octa-β-ala-octa-*O*-propoxycalix[8]arene trifluoroacetic salt (3). ^{1}H NMR: (400 MHz, MeOD, 330 K) δ 0.74 (t, $J = 7.2$ Hz, CH_3, 24H), 1.56 (m, CH_2, 16H), 2.69 (br t, CH_2CO, 16H), 3.19 (t, $J = 6.5$ Hz, OCH_2, 16H), 3.48 (br t, $CH_2NH_3^+$, 16H), 3.95 (br s, $ArCH_2Ar$, 16H), 7.23 (s, ArH, 16H). ES-MS calcd for $C_{104}H_{145}O_{16}N_{16}$ 1875.4016 ($M+H^+$). Found 1874.7.

4.3.2. Octa-lys-octa-*O*-propoxycalix[8]arene trifluoroacetic salt (4). ^{1}H NMR (400 MHz, DMF-d_6, 297 K) δ 0.78 (t, $J = 7.2$ Hz, CH_3, 24H), 1.59 (m, $2 \times CH_2$, 32H), 1.79 (m, CH_2, 16H), 2.02 (m, CH_2, 16H), 3.03 (t, $J = 6.5$ Hz, OCH_2, 16H), 3.53 (m, $CH_2NH_3^+$, 16H), 3.98 (br s, $ArCH_2Ar$, 16H), 4.23 (br t, $J = 6.2$ Hz, CH, 8H), 7.45 (s, ArH, 16H), 8.42 (br s, NH_3^+, 24H), 8.78 (br s, NH_3^+, 24H), 10.61 (s, NH, 8H). ES-MS calcd for $C_{128}H_{201}O_{16}N_{24}$ 2332.1672 ($M+H^+$). Found 2331.2.

4.3.3. Octa-6-amino-hexanoic-octa-*O*-propoxycalix[8]-arene trifluoroacetic salt (5). ^{1}H NMR (400 MHz, MeOD, 297 K) δ 0.80 (t, $J = 7.2$ Hz, CH_3, 24H), 1.40 (m, CH_2, 16H), 1.45 (m, CH_2, 16H), 1.55 (m, $2 \times CH_2$, 32H), 2,31 (t, $J = 7.1$ Hz, CH_2CO, 16H), 2,92 (t, $J = 7.5$ Hz, OCH_2, 16H), 3.51 (br t, $CH_2NH_3^+$, 16H), 3.96 (br s, $ArCH_2Ar$, 16H), 7.22 (s, ArH, 16H). ES-MS calcd for $C_{128}H_{193}O_{16}N_{16}$ 2211.0416 ($M+H^+$). Found 2210.3.

4.3.4. Octa-8-amino-octanoic-octa-*O*-propoxycalix[8]-arene trifluoroacetic salt (6). ^{1}H NMR (400 MHz, MeOD, 297 K) δ 0.79 (t, $J = 7.1$ Hz, CH_3, 24H), 1.37 (m, $3 \times CH_2$, 48H), 1.56 (m, $3 \times CH_2$, 48H), 2.26 (t, $J = 7.5$ Hz, CH_2CO, 16H), 2.88 (t, $J = 7.4$ Hz, OCH_2, 16H), 3.51 (br t, $CH_2NH_3^+$, 16H), 3.96 (br s, $ArCH_2Ar$, 16H), 7.20 (s, ArH, 16H). ES-MS calcd for $C_{144}H_{225}O_{16}N_{16}$ 2540.4712 ($M+H^+$). Found 2539.7.

4.4. Experimental conditions for kinetic measurements

In order to measure kinetic constant K_m for the hydrolysis of the substrate Tosyl-Gly-Pro-Arg-*p*-nitroanilide (GPR-*p*NA) by recombinant human lung tryptase, kinetic experiments, according to the slightly modified procedures of Tanaka et al.[28] were made. Working stock solution of 10 nM enzyme in 10 mM MES (pH 6.1) containing 2 N NaCl was prepared. Kinetic experiments were carried out in 50 mM Tris–HCl buffer, pH 8.0, and 0.02% Triton-X, at 25 °C in a final volume of 900 μL.

Tryptase activity (45 μL of stock solution, final concentration of enzyme and NaCl 0.5 nM and 0.1 N, respectively) was tested in the above buffer at 25 °C, with different concentration of GPR-*p*NA as substrate (ranging from 80 to 320 μM), monitoring the change of absorbance at 405 nm. The K_m for GPR-*p*NA substrate (1.5 mM ± 0.34) was determined using Lineweaver–Burk analysis. Inhibition assays were carried out at 25 °C in the above condition adding the fixed amount of enzyme to a solution 50 mM Tris–HCl buffer, 0.02 % Triton-X, pH 8.0, containing a substrate concentration of 240 μM, and inhibitors **3**–**6** at different concentration (ranging from 5 to 500 nM). The change of absorbance at 405 nm was monitored over a period of 45 min. The experiments were repeated at least three times with each inhibitor.

4.5. Dynamic light scattering measurements

Quasi-elastic light-scattering (QELS) measurements were performed by using a computerized homemade goniometer and the exciting light source was a 200 mW polarized Nd: YAG laser (532 nm). The investigated scattering angle was 90°. The scattered light was collected, in a self beating mode, through an optical fiber matched with a digital Hamamatsu R942 photomultiplier cooled at −30 °C. The signal was sent to a Malvern 4700 submicrometer particle analyzer system in homodyne

detection mode. The measured scattered intensity of the solutions were normalized by the scattered intensity of toluene used as reference and the percentage of aggregated molecules was estimate (<0.001% in a range of concentrations from 10^{-3} to 10^{-6} M). Hydrodynamic radius R_H of the aggregate molecules was deduced through the Einstein–Stokes relation.

Acknowledgements

We thank Dr. Fulvio Erba, University of Rome 'Tor Vergata', for the helpful suggestion on recombinant tryptase. Drs. Norberto Micali and Valentina Villari, IPCF-CNR sez. of Messina, for light scattering measurements and Dr. Rita La Spina for careful contribution to the kinetic measurements and calculations.

References and notes

1. Peczuh, M. W.; Hamilton, A. D. *Chem. Rev.* **2000**, *100*, 2479.
2. Park, H. S.; Lin, Q.; Hamilton, A. D. *J. Am. Chem. Soc.* **1999**, *121*, 8.
3. Hamuro, Y.; Calama, M. C.; Park, H. S.; Hamilton, A. D. *Angew. Chem., Int. Ed.* **1997**, *36*, 2680.
4. Blaskovich, M. A.; Lin, Q.; Delarue, F. L.; Sun, J.; Park, H. S.; Coppola, D.; Hamilton, A. D.; Sebti, S. M. *Nat. Biotechnol.* **2000**, *18*, 1065.
5. Jain, R. K.; Hamilton, A. D. *Org. Lett.* **2000**, *2*, 1721.
6. Jain, R. K.; Hamilton, A. D. *Angew. Chem., Int. Ed.* **2002**, *41*, 641.
7. Fischer, N. O.; McIntosh, C. M.; Simard, J. M.; Rotello, V. M. *Proc. Natl. Acad. Sci. U.S.A.* **2002**, *99*, 5018.
8. Hong, R.; Fischer, N. O.; Verma, A.; Goodman, C. M.; Emrick, T.; Rotello, V. M. *J. Am. Chem. Soc.* **2004**, *126*, 739.
9. Caughey, G. H. *Mast Cell Proteases in Immunology and Biology*; Marcel Dekker: New York, 1995.
10. Caughey, G. H. *Am. J. Respir. Cell. Mol. Biol.* **1997**, *16*, 621.
11. Clark, J. M.; Abraham, W. M.; Fishman, C. E.; Forteza, R.; Ahmed, A.; Cortes, A.; Warne, R. L.; Moore, W. R.; Tanaka, R. D. *Am. J. Respir. Crit. Care Med.* **1995**, *152*, 2076.
12. Clark, J. M.; Moore, W. R.; Tanaka, R. D. *Drugs Future* **1996**, *21*, 811.
13. Maryanoff, B. E. *J. Med. Chem.* **2004**, *47*, 769.
14. Pereira, P. J. B.; Bergner, A.; Macedo-Ribeiro, S.; Huber, R.; Matschiner, G.; Fritz, H.; Sommerhoff, C. P.; Bode, W. *Nature* **1998**, *392*, 306.
15. Sommerhoff, C. P.; Bode, W.; Pereira, P. J. B.; Stubbs, M. T.; Stürzebecher, J.; Piechottka, G. P.; Matschiner, G.; Bergner, A. *Proc. Natl. Acad. Sci. U.S.A.* **1999**, *96*, 10984.
16. Alter, S. C.; Metcalfe, D. D.; Bradford, T. R.; Schwartz, L. B. *Biochem. J.* **1987**, *248*, 821.
17. Schwartz, L. B.; Bradford, T. R. *J. Biol. Chem.* **1986**, *261*, 7372.
18. Addington, A. K.; Johnson, D. A. *Biochemistry* **1996**, *35*, 13511.
19. Sommerhoff, C. P.; Sollner, C.; Mentele, R.; Piechottka, G. P.; Auerswald, E. A.; Fritz, H. *Biol. Chem. Hoppe Seyler* **1994**, *375*, 685.
20. Rice, K. D.; Tanaka, R. D.; Katz, B. A.; Numerof, R. P.; Moore, W. R. *Curr. Pharm. Des.* **1998**, *4*, 381.
21. Costanzo, M. J.; Yabut, S. C.; Almond, H. R.; Andrade-Gordon, P.; Corcoran, T. W.; de Garavilla, L.; Kauffman, J. A.; Abraham, W. M.; Recacha, R.; Chattopadhyay, D.; Maryanoff, B. E. *J. Med. Chem.* **2003**, *46*, 3865.
22. Burgess, L. E.; Newhouse, B. J.; Ibrahim, P.; Rizzi, J.; Kashem, M. A.; Hartman, A.; Brandhuber, B. J.; Wright, C. D.; Thomson, D. S.; Vigers, G. P. A.; Koch, K. *Proc. Natl. Acad. Sci. U.S.A.* **1999**, *96*, 8348.
23. (a) Gutsche, C. D. *Calixarenes*; Royal Society of Chemistry: Cambridge, 1989; (b) Gutsche, C. D. *Calixarenes Revisited*; Royal Society of Chemistry: Cambridge, 1998.
24. Neri, P.; Consoli, G. M. L.; Cunsolo, F.; Geraci, C.; Piattelli, M. In *Calixarenes 2001*; Asfari, Z., Böhmer, V., Harrowfield, J., Vicens, J., Eds.; Kluwer Academic: Dordrecht, 2001; pp 89–109.
25. Verboom, W.; Durie, A.; Egberink, R. J. M.; Asfari, Z.; Reinhoudt, D. N. *J. Org. Chem.* **1992**, *57*, 1313.
26. Hallgren, J.; Estrada, S.; Karlson, U.; Alving, K.; Pejler, G. *Biochemistry* **2001**, *40*, 7342.
27. Niles, A. L.; Maffitt, M.; Haak-Frendscho, M.; Wheeless, C. J.; Johnson, D. A. *Biotechnol. Appl. Biochem.* **1998**, *28*, 125.
28. Tanaka, T.; McRae, B. J.; Cho, K.; Cook, R.; Fraki, J. E.; Johnson, D. A.; Powers, J. C. *J. Biol. Chem.* **1983**, *285*, 13552.
29. Copeland, R. A. *Enzymes: a Practical Introduction to Structure, Mechanism, and Data Analysis*, 2nd ed.; Wiley-VCH: New York, 2000.
30. Morrison, J. F.; Walsh, C. T. *Adv. Enzymol.* **1988**, *61*, 201.
31. Shinkai, S.; Arimura, T.; Araki, K.; Kawabata, H. *J. Chem. Soc., Perkin. Trans. 1* **1989**, 2039.
32. Munch, J. H.; Gutsche, C. D. *Org. Synth.* **1989**, *68*, 243.